Trends in the electric quadrupole fields at dilute impurity sites in transition-metal—transition-metal alloys

R. E. Watson and R. M. Sternheimer
Physics Department, Brookhaven National Laboratory, Upton, New York 11973

L. H. Bennett
National Bureau of Standards, Washington, D.C. 20234

(Received 21 March 1984)

The available electric-field-gradient data at transition-metal impurity sites and at host sites in transition-metal hosts has been inspected for indications of trends in alloying behavior. The raw data separate the gradients into two groups, depending on whether the host metal has over, or under, half-filled d bands. The gradients for any given probe atom are largely independent of which host, in a given group, is involved, running counter to simple chemical intuition. Analysis is complicated by various intra- and inter-atomic contributions to the field gradient and the practice has been adopted of presuming that one or another contribution prevails and normalizing the experimental data by an effective field appropriate to the probe atom and to the contribution involved. The normalized results suggest that the observed gradients, by their very magnitude, must be largely intra-atomic in origin. Granted this, and assuming that it is the d electrons which are primarily responsible, we find that, while there is scatter in the data, the gradients at host and impurity sites, in the under-half-filled d-shell hosts, show little chemical variation with either differing impurity or differing host. The normalized results for the over-half-filled d-shell hosts, on the other hand, appear to show a chemical trend which is also to be seen in the enthalpies of formation of the more concentrated alloys. The normalizations, if we assume intra-atomic effects, required estimates of the field gradient due to a single valence electron. The renormalized-atom scheme was employed to obtain the contributions from d- and valence p-electron charge. It is not widely appreciated as to how important p-electron bonding can be to the gradients. Sternheimer antishielding factors, γ_∞, were also required. Lacking values for some of the elements of concern, a simple scaling with the size of the atom was introduced. This was inferred from a number of sequences of ions and then applied to predictions for the $5d$ elements. The scaling worked well and should do so in other cases as well.

I. INTRODUCTION

Measurements of hyperfine fields provide a valuable probe of the environments in which atoms find themselves in solids and in molecules. Knight shifts and Mössbauer isomer shifts, for example, show whether an atomic species is in more than one type of site in a sample, and, from the distribution of the shifts, indicate the distribution of sites. The isomer shifts are a measure of charge transfer. Quadrupole effects are a measure of the aspherical charge density around an atomic site, and, as such, are indicative of directional chemical bonding. Of concern in the present paper are the properties of transition-metal impurities in transition-metal hosts. There is considerable experimental data concerning impurity isomer shifts, particularly for the $5d$ elements, indicating[1] a systematic variation in the relative roles of d- and non-d-electron bonding effects, as a transition-metal row is traversed, i.e., as one transition-metal impurity is replaced by another in a sequence of transition-metal hosts. Only recently has there become experimental data[2–9] to allow a similar scan of quadrupole field gradients, eq_{expt}. Hagn and coworkers have, for example, obtained[2] results for a significant number of $5d$ impurities in Lu and Re hosts (Fig. 1) showing disparate behavior between the two hosts. One purpose of that work was to test the proposal[10] of Raghavan *et al.* that the ratio of inter- to intra-atomic contributions to the impurity field gradient is a universal constant. Hagn *et al.* concluded that the results represented in Fig. 1 are inconsistent with this proposal. Granted the dif-

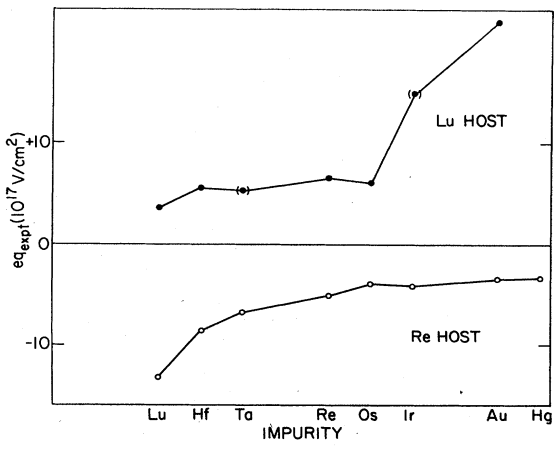

FIG. 1. Field gradients for various $5d$ atoms in Lu and Re hosts as reported (Ref. 2) by Hagn *et al.* Parentheses indicate cases where the sign of a gradient was not determined.

ferent trends in eq_{expt} for Lu and Re hosts, there naturally arises the question of what, if any, overall trend occurs in field-gradient behavior when other hosts are considered as well. This issue is addressed here.

When discussing the trends in eq_{expt}, it will be useful to divide the field gradient into three terms, rather than the two alluded to above, namely

$$eq = eq_{\text{intra}} + eq_{\text{LR}} + eq_{\text{inter}} \ . \tag{1}$$

The first term is the intra-atomic contribution arising from the aspherical character of the valence charge within the impurity atomic cell. The second is the long-range (LR) inter-atomic contribution involving a lattice sum over the host crystal. For a hexagonal-close-packed lattice, its leading term has the form[11]

$$V_{\text{LR}} = \frac{ne}{a^3}[0.0065 - 4.3584(c/a - 1.633)] \ , \tag{2}$$

where ne is the effective charge at a host site and c and a are the hcp lattice constants (we presume, as others have, that the impurity is at a substitutional site). The third term, which is sometimes neglected and sometimes partitioned between the other two, involves those inter-atomic contributions associated with the disturbance due to the impurity in the immediate surrounding host medium. This may involve charge transfer, changes in directional bonding, and shifts[9] in near-neighbor nuclear positions. At first, it would seem that the eq_{expt} of large magnitude in Fig. 1 are associated with alloys where there is strong chemical bonding between the impurity and the host. This is the case for Au and Ir alloyed into Lu, but the bonding is much weaker when Lu is alloyed into Re. In these three alloys the mismatch in atomic volumes is known to distort the host lattice in the vicinity of the impurity. However, there are substantial volume mismatches between Lu and *all* the other elements displayed in the figure. It would appear that the trends seen in Fig. 1 cannot be blamed in a simple way on variations in bonding and its effects on q_{inter}. The individual terms of Eq. (1), of course, involve the appropriate Sternheimer antishielding factors,[12–19] with the largest antishielding associated with the long-ranged term. Despite being multiplied by a large factor, it will be seen in the next section that eq_{LR} is 1 or 2 orders of magnitude smaller than the experimentally observed gradients, and it therefore is the first and third terms of Eq. (1) which are responsible for the observed gradients.

The use of experimental hyperfine fields as a measure of transition-metal alloying largely ends up being a study of $5d$ impurities because it is these elements which have suitable nuclear states. This is true for the isomer shifts[1] as well as for the quadrupole field gradients of concern here. Among the $3d$ and $4d$ elements, there is significant data for only Fe and Ru, although, in the case of Ru, the sign of eq is not known for any of the data. One may, of course, scan for the effects on $5d$ impurities in going from $5d$ to $4d$ and, in turn, $3d$, noncubic metal hosts. This will be done.

The plan of the paper is as follows. Several quantities relevant to the individual terms of Eq. (1) are estimated in Sec. II. These include the lattice term eq_{LR} and "renormalized-atom" values of the quadrupole fields, eq_d, associated with single d electrons. The latter serve to set the scale of the intra-atomic effects to be expected from the d bands. Valence $6p$-electron quadrupole terms will also be reported for several of the $5d$ metals, for there is $6p$ character in their conduction bands, and it is not generally appreciated as to how large the associated field-gradient contributions can be. Sternheimer antishielding factors will be required, and these are, as a rule, not available for the $5d$ transition elements. The Appendix explores the variation in the external antishielding factor, γ_∞, as a function of the size of the atom involved for sequences of atoms for which there is data. This suggests a scaling rule, which is then used in Sec. II to estimate the variation in γ_∞ across the $5d$ row. No attempt will be made to perform full metallic calculations, either involving just Fermi-surface repopulation effects,[20] or the more detailed model scheme[21] of Piecuch and Janot, which has had mixed success[5] in predicting field gradients in metals. The problem is that a detailed calculation should account for the host-lattice distortion around the impurity site and for any valence p-electron contributions to the field gradient. This is difficult; however, as will be suggested in the conclusion, some full-scale energy-band predictions of eq in the elemental metals would be of considerable use. Figure 1 is extended to include experimental data for the $5d$ impurities in other $5d$ hosts in Sec. III. Also shown are plots of the impurity field gradient for Fe, Ru, and those $5d$ elements for which there is $3d$ and $4d$, as well as $5d$, host data. As is the case in Fig. 1, it is necessary to make assumptions concerning the sign of an eq_{expt} when the sign is not known (the data points in such cases are drawn in parentheses). The plots in Sec. III include all the transition-metal–transition-metal impurity field gradients that we have found for which the sign is known, and all but a dozen scattered cases for which the magnitude but not the sign is known. These results will be "normalized" in Sec. IV by dividing by, on one hand, the intra-atomic d-orbital eq_d, and, on the other hand, dividing by the external Sternheimer antishielding factor γ_∞. The relation of the raw and the normalized gradients to alloy-bonding trends is discussed in Sec. V.

Granted the scatter and the uncertainty in sign of some of the experimental gradients, it will be seen that all the individual eq_{expt} fall on one or the other of the two curves defined[2] by Hagn *et al.*, Fig. 1, which curve depends on whether the host metal has under- or over-half-filled d bands. Inspection of the normalized gradients suggest that there is surprisingly little variation in chemical behavior for the various impurities in the various hosts belonging to one or the other of the two groups.

II. NUMERICAL CONSIDERATIONS

An impurity-site field gradient involves factors which are properties of the impurity atom and factors which depend on the interaction of the impurity with its surroundings. It is useful to differentiate between the two. The intra-atomic term, for example, depends on the radial character of the impurity-bonding electrons. A measure of this is the field gradient due to a single $m_l = 0$ valence

orbital. For a d electron, this is

$$eq_d = 9.718(\tfrac{4}{7})e\langle r^{-3}\rangle_d \ , \tag{3a}$$

where $\frac{4}{7}$ is the angular integration factor, $\langle r^{-3}\rangle$ is the r^{-3} expectation value of the radial d orbital, and the prefactor is chosen so that the gradient is in units of 10^{17} V/cm^2; $\langle r^{-3}\rangle$ is in units of a_0^{-3}, where a_0 is the Bohr radius. The equivalent expression for an $m_l=0$ valence p electron is

$$eq_p = 9.718(\tfrac{4}{5})e\langle r^{-3}\rangle_p \ . \tag{3b}$$

The values of q_d for Fe, Ru, Zr, and the $5d$ elements in Table I were obtained with a renormalized-atom scheme where the orbitals were calculated with free-atom boundary conditions, but then renormalized inside the atomic Wigner-Seitz sphere, appropriate to the elemental metal, on each iteration of the self-consistent calculation. This normalization makes sense inasmuch as valence-charge counts in metals are normally made in terms of the charge within the atomic cell. Values of q_p are also quoted in the table for several of the $5d$ elements where calculations were done for the $5d^n6p^1$ configurations (those for the q_d involved d^ns^1 configurations, which are the closest integral assignments to the configurations appropriate to the metals). The calculations were done in the relativistic Dirac-Fock scheme where j is a good quantum number and $\langle r^{-3}\rangle_d$ is a weighted average of the $\langle r^{-3}\rangle$ of the $j=\frac{3}{2}$ and $\frac{5}{2}$ $5d$ subshells, while $\langle r^{-3}\rangle_p$ was taken to be that of a $j=\frac{3}{2}$ orbital. Based on relativistic calculations, these assignments are not entirely consistent with insertion into Eqs. (3), but serve to set the scale of the intra-atomic field-gradient contributions. It is useful to divide the experimental gradients by these quantities,

$$\xi_i \equiv \frac{q_{\text{expt}}}{q_i} \ , \tag{4}$$

after the manner of Knight's treatment[22] of Knight shifts where he divided the hyperfine field associated with observed shift by the hyperfine field appropriate to the atom in question. The resulting ξ for a Knight shift is then a measure of band-structure effects. Here it would be more appropriate to replace the full gradient q_{expt} by the intra-atomic term alone. Lacking separate values for the terms in Eq. (1), this cannot be done, and it will prove of interest to inspect Eq. (4).

TABLE I. Field gradients eq_d and eq_p associated with $m_l=0$ renormalized valence-electron orbitals [see Eqs. (3)] in 10^{17} V/cm^2. Also listed are $5d$-element γ_∞ antishielding factors, extrapolated off the value for Au with Eqs. (6a) and (6b).

	eq_d	eq_p	$-\gamma_\infty$[a]	$-\gamma_\infty$[b]
La	10.9			
Lu	14.1	113.0	136.0	103.0
Hf	21.8		92.0	81.0
Ta	28.2	202.0	69.0	67.0
W	34.8		59.0	61.0
Re	41.9		54.0	58.0
Os	49.4	245.0	51.0	57.0
Ir	57.2		54.0	59.0
Pt	65.4		61.0	64.0
Au	77.5	195.0	74.2	74.2
Fe	24.0			
Ru	28.2			
Zr	13.0			

[a]Equation (6a).
[b]Equation (6b).

Table I indicates that q_p is some 8 times larger than q_d for the lighter transition metals, falling off to a factor of 2.5 for Au. It would appear that a small amount of p character, concentrated along a bond line, can make a large contribution to the gradient—compare the q_p of the table with the magnitudes of the experimentally measured gradients in Fig. 1. The q_p would be substantially smaller if given in terms of free-atom orbitals whose charges reside largely outside the atomic Wigner-Seitz cells, and, in fact, much of the discussion of p gradient effects in the literature has employed that normalization. However, according to band-theory results,[23] there is one-half to two-thirds of an occupied p electron's worth of charge, in the conduction bands and hybridized into the d bands, which is *within* the Wigner-Seitz cell of a transition metal. The q_p of Table I are appropriate when estimating the gradient arising from any asphericity in this charge, and, due to the size of the q_p, this asphericity need not be much to have an observable effect. The importance of this to gradients measured in Au compounds has been discussed elsewhere.[24]

The Sternheimer antishielding factor is a measure of the closed-shell distortion of an atom in the presence of a quadrupole field, and, in turn, the contribution of that distortion to the gradient sampled by the nucleus. As such, antishielding, like the intra-atomic q_d and q_p, is intrinsic to the impurity atom. The antishielding of the intra-atomic terms is modest because of the overlap between the valence and the closed shells. Typically, it leads to a 30% enhancement of these gradients and may be considered constant across the $5d$ row for our purposes here. The situation is quite different for the Sternheimer antishielding γ_∞ associated with a perturbing potential originating outside the atom. There are calculated γ_∞ values[18] for W and Au atoms of -57 and -74.2, respectively (it is $1-\gamma_\infty$ that multiplies the unshielded field gradient). The value for W is expected to be an underestimate since the contribution from the open $5d$ shell was not included. The observations in the Appendix suggest a size-dependent interpolation scheme for obtaining γ_∞ for the other $5d$ elements. There it is observed that sequences of atoms, from the same column of the Periodic Table and having the same outer configuration of valence electrons, have γ_∞ values which vary, *on the average*, as $R^{4.5}$, where R is Slater's atomic radius.[25] This would suggest that

$$\frac{\gamma_\infty(A)}{\gamma_\infty(B)} = \left[\frac{V(A)}{V(B)}\right]^{1.5} \tag{5}$$

for the ratio for elements A and B, where the V's are their volumes. (As is discussed in the Appendix, a positive exponent such as this is expected, but its magnitude is surprisingly large.) This fit, involving ions of common

valence-electron counts, is not directly applicable to the case at hand involving ions with varying d-electron counts across a transition-metal row. However, the d contribution is expected to vary linearly with the d occupation, and, noting that roughly 25% of the calculated γ_∞ for Au comes from the $5d$ shell, this suggests that

$$\gamma_\infty(B)=\gamma_\infty(\mathrm{Au})[0.75+0.25(n/10)][V(B)/V(\mathrm{Au})]^{1.5}\ , \tag{6a}$$

where n is element B's d count (we have used integral values). The resulting γ_∞ are listed in Table I. The interpolated result for W is slightly larger than the value, -57, which was calculated[18] neglecting the $5d$ shell, although this difference is less than might be expected. On the other hand, the results for Lu and Hf are larger than would be expected, granted that γ_∞ values such as -80 are typical[16] for trivalent rare earths such as Tm^{3+}, and -93 has been calculated[19] for divalent Yb^{2+}, which is next to Lu in the Periodic Table. Inspection of the fits in the Appendix suggests that the exponent of Eqs. (5) and (6a) has been inflated by a core-screening effect, which is not relevant for scaling for size, and that an exponent closer to 1, i.e.,

$$\gamma_\infty(B)=\gamma_\infty(\mathrm{Au})[0.75+0.25(n/10)][V(B)/V(\mathrm{Au})]^{1}\ , \tag{6b}$$

is more appropriate. Extrapolated values of γ_∞ with this exponent are listed in the final column of Table I. These γ_∞ are in good accord with expectations for Lu, Hf, and W, and the changes in value associated with the change in exponent are only substantial for Lu and Hf. The results of Eq. (6b) will be used in Sec. IV. Such extrapolations not only work well in providing values of γ_∞, which are not otherwise available, but they offer insight into the dependence of γ_∞ with varying state of ionization and with differing atomic number.

The γ_∞ described above is appropriate to the long-ranged field gradient contribution for which Eq. (2) is the leading term. This term is near-zero-valued because we are dealing with monatomic host metals where each atomic Wigner-Seitz cell is neutrally charged, hence $n_e=0$. However, the Wigner-Seitz cells themselves are not spherical, nor are the charge distributions within them, and this leads to multipole contributions to the field gradient at the impurity site. Often these are estimated by approximating the crystal by an array of spherical "point" charges in a compensating uniform electron-charge background. Instead, these may be calculated with Fourier transforms or with the bipolar expansion.[26] The contributions from higher multipoles fall off very rapidly with distance and, crudely speaking, they make a contribution of the order of 0.1 or less to an *effective* spherical charge which might be inserted into Eq. (2). Evaluating Eq. (2) with this and multiplying the result with an antishielding factor of 100 (which is a reasonable upper bound), eq_{LR} ranging from 0.05 to 0.17 (10^{17} V/cm^2) for Gd, Lu, Hf, Re, and Os hosts are obtained. These are 1—2 orders of magnitude smaller than the experimental field gradients seen in Fig. 1. In other words, if it were assumed that the observed gradients were, in fact, primarily due to eq_{LR}, then effective spherical site charges of 1 to 10 [the n of Eq. (2)] would be required, and this is out of the question in the metallic systems of concern here. Experimental gradients of the scale seen here thus arise from the impurity site and its immediate surroundings[21] and not from long-range terms.

The appropriate Sternheimer antishielding factor for eq_{inter}, the inter-atomic terms coming from the immediate surroundings, is not γ_∞. This is because of overlap between the surrounding charge distribution and the tails of the impurity-site orbitals. These tails contribute importantly to the large values of the γ_∞'s and overlap reduces their contribution. Recent detailed calculations[17] for Fe in Fe_2O_3 indicate that such antishielding is reduced to roughly one-third of the γ_∞ value. The exact amount of the reduction will not be important here and the assumption is made that the reduction is roughly constant across the $5d$ transition-metal row.

III. TRENDS IN EXPERIMENTAL FIELD GRADIENTS

The available experimental impurity field-gradient data for the noncubic $5d$ hosts Gd, Hf, and Os, in addition to that for Lu and Re, are shown in Fig. 2. (Also shown is the observed gradient for La in La, the only data with La as host. La is the one double hcp metal considered here. The local atomic environment is such that it is appropriate to compare the La results with the other, hcp, cases.) Noting their positions in the Periodic Table, one might have expected the Gd-host data points to lie above those for Lu, with those for Hf lying between Lu and Re, but close to Lu, and with the Os data to the far side of Re. Instead, the data appear clumped in two disparate trends, with that for the under-half-filled $5d$-band host metals La, Gd, Lu, and Hf in one curve, and the heavier host metals Re and Os in another, better defined curve. Some uncertainty must be attached to individual plotted points. Among other things, values of some of the nuclear quad-

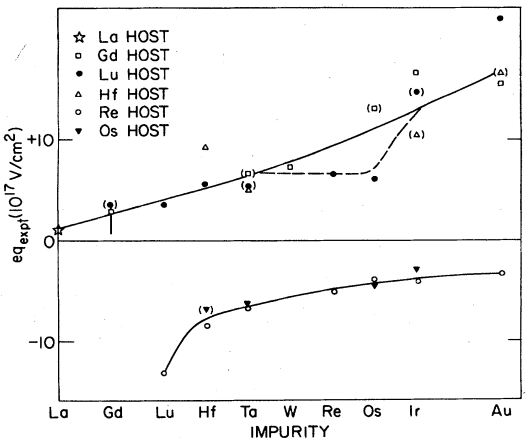

FIG. 2. Field gradients eq_{expt} observed for various $5d$ atoms in various $5d$ hosts. Parentheses indicate cases where the sign of the gradient was not determined. The lines have been drawn to guide the eye. The vertical line indicates the spread in reported values for Gd in Gd.

rupole moments are not well established and not all measurements were done at a common temperature. Gd in Gd is an extreme example of the problem: There is a factor-of-6 spread in the various reported experimental eq values which is indicated by the vertical line in the figure. This is not simply due to temperature effects since there are high- and low-temperature data close to both the top and the bottom of the line. Not involving the implanting of an impurity in another host, these results should be relatively insensitive to details of sample preparation. Unfortunately, there is no discussion in the literature concerning the disagreement from one experiment to another. In other cases where there is more than one experimental evaluation[7] of eq, there is sometimes rough agreement, and sometimes not.

Lines have been drawn freehand to guide the eye in Fig. 2. Details depend on how smooth a curvature one demands, but, for the most part, it is easy to draw curves, summarizing the trends in the eq_{expt}, through the data. The exception occurs in the vicinity of Re and Os, as impurities in the lighter hosts, where a glitch, as indicated by the dashed line, summarizes the data equally well.

There are experimental data for Fe and Ru as impurities and for some of the $5d$ impurities of Fig. 2 in $3d$ and $4d$ transition-metal hosts. In contrast with Fig. 2, it is convenient to plot eq_{expt} for a given impurity as a function of the column in the Periodic Table in which the host belongs. This is done for Fe and Ru in Figs. 3 and 4. Note that the signs of eq_{expt} are unknown for all the Ru data and for most of those associated with the left-hand hosts of Fe. In such cases, gradient is plotted assuming that its sign is consistent with the trend indicated in Fig. 2, i.e., positive values for host metals with less-than-half-filled d bands and negative for those, over-half-filled, to their right. Note the data point for Fe in Ti which is small in magnitude but of opposite sign to the general trend: It is the one case in all of the data to be of "wrong" sign. The magnitudes of the Fe gradients differ from those tabulated in the literature. After the last collection of data, Duff and co-workers performed detailed calculations[27] for molecular $FeCl_2$ and $FeBr_2$, including estimates of the gradients at the Fe nuclei. Upon comparison with experiment, a Q value of $0.082b$ was obtained for ^{57}Fe, in contrast with the previously accepted value of ~ 0.20. Support was given to this assignment by Vajda and co-workers who took[28] the quadrupole moment for ^{54}Fe obtained from a nuclear-shell-model calculation, which was believed to be reliable, and scaled it by the known ratio of moments for the two nuclei, obtaining almost exactly the same value as Duff *et al.* The gradients of Fig. 3 have been scaled to account for the newly assigned value of $Q(^{57}\text{Fe})$, and the comparisons of the next section lend further support to this assignment. It might be noted that the magnitudes of the Fe- and Ru-site gradients appearing in Figs. 3 and 4 are, on the average, smaller than those for Os and the adjacent $5d$ elements in Fig. 2.

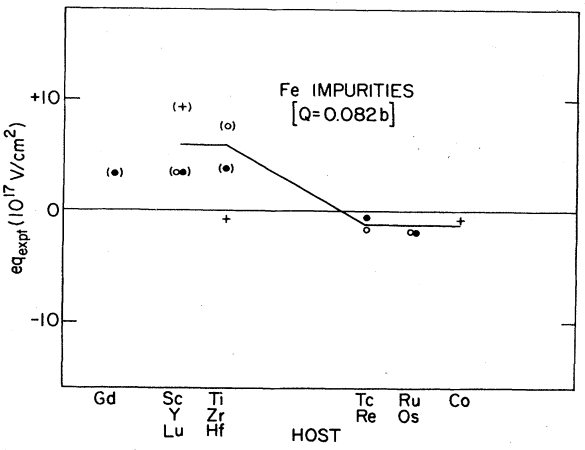

FIG. 3. Field gradients eq_{expt} for Fe in various transition-metal hosts. The gradients were obtained assuming the ^{57}Fe quadrupole moment as estimated in Refs. 27 and 28. Pluses indicate $3d$; open circles, $4d$; and solid circles, $5d$ hosts. The signs of the gradients were not determined for those cases in parentheses. The lines have been drawn to guide the eye.

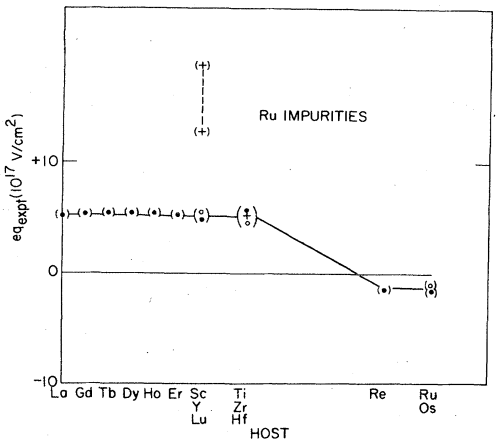

FIG. 4. Field gradients eq_{expt} for Ru in various transition-metal hosts following the conventions of Fig. 3. Note that the sign of the field gradient is known for none of the Ru data.

Data for Gd, Hf, Ta, Ir, and Au in $3d$ and $4d$, as well as $5d$, hosts are summarized in Fig. 5. The horizontal lines are not drawn through the data, but have their positions equal to the values of the curves in Fig. 2 which are appropriate to the impurity in question. Thus, the extent to which all the data, for some impurity, lie on the pair of lines is a measure of how well the gradients can be characterized as having but one of two values, depending on the class of host. This works well for Ta and Gd impurities and reasonably well for Hf, but less well for Ir and Au in the left-hand hosts where there is substantial scatter in the data and where there is the distinct suggestion, particularly for Ir in Ti, Zr, and Hf, that these hosts are acting intermediate between those to their left and to their right, rather than acting like those to their left. There are other breaks[29] with the pairs of flat lines, e.g., the eq_{expt} with Re as host tend to be somewhat larger than those associated with Os and Ru, and, in turn, Co. This variation is weak on the scale of the disparity in eq_{expt} for right- and for left-hand hosts. Assuming that no mistakes were made in the assignment in the signs of some gradients, all the data fall quite well on the two curves originally defined[2] by Hagn and co-workers for Lu and Re hosts. The

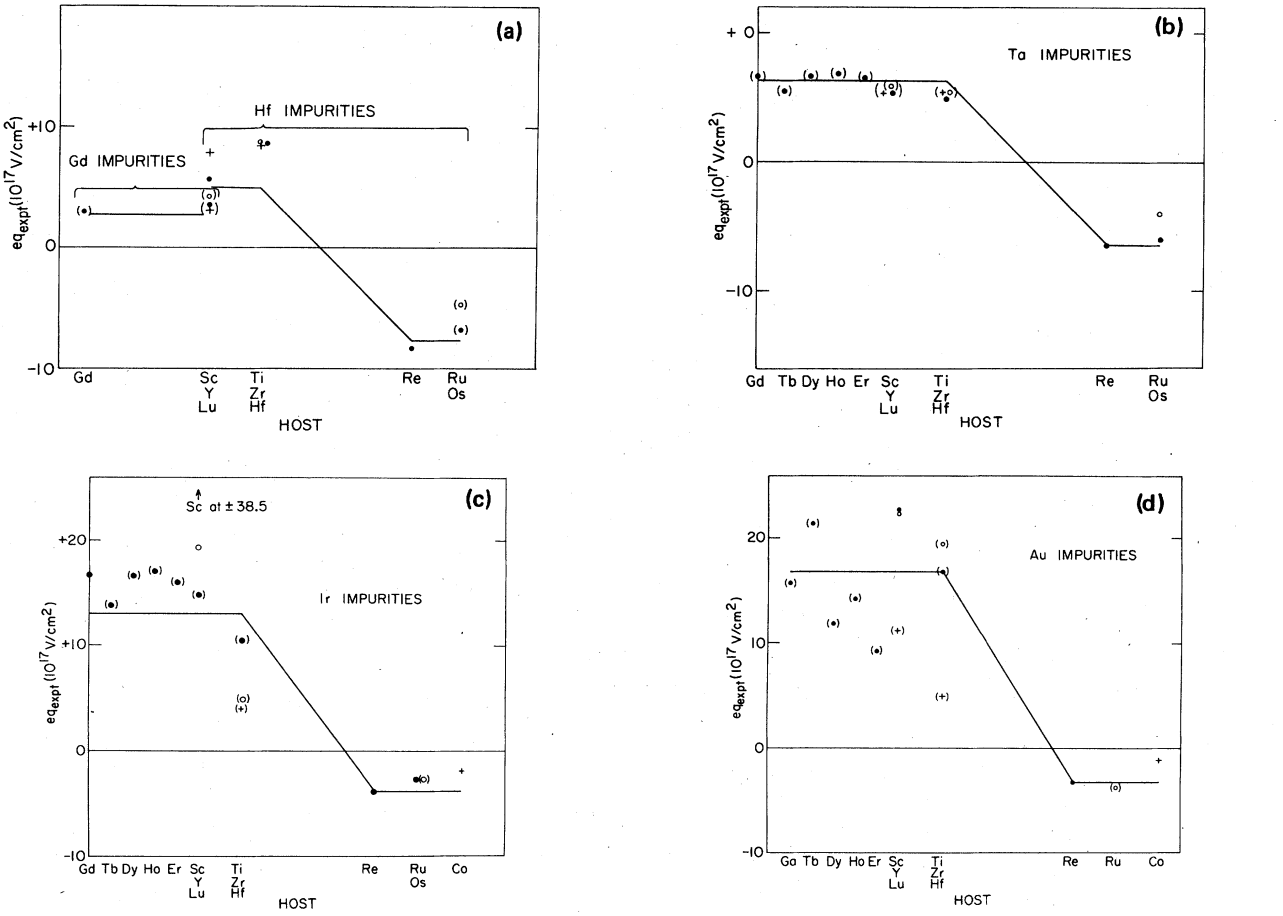

FIG. 5. Field gradients observed for Gd, Hf, Ta, Ir, and Au atoms in various transition-metal hosts. The conventions of Fig. 3 are followed *except* that the positions of the horizontal lines are set by the values from the two curves in Fig. 2 for the impurity atom in question.

extent to which this is so is remarkable granted the variation in size and in chemical behavior within each group of hosts. In the next section we will see that the Fe and Re data fall in well with that for the $5d$ impurities.

IV. NORMALIZED GRADIENTS

Simple inspection of Figs. 1–5 does not allow one to differentiate between the effects associated with alloying, which are of interest, and those due to the atomic properties of the impurity in question. It would be desirable to be able to divide out any atomic factors so that the remainder simply reflect alloying effects. This cannot be done with rigor since there is more than one contribution to the gradient, i.e., the inter- and intra-atomic terms of Eq. (1). One approach is to assume that the intra-atomic contributions dominate and inspect the ξ_d factor as defined in Eq. (4). This is done for the field gradients associated with $5d$ hosts in Fig. 6. There are several features of the behavior of the ξ_d which deserve attention.

First, while there is the indication of a systematic variation in the ξ_d of La, Gd, Lu, and Hf in *their own* host lattices,[30] all the impurity data associated with these hosts lie in a rather well-defined band. This band has a *constant* position with varying impurity. There is significant scatter of the ξ_d within the band, causing it to have significant breadth, as is sketched by the hatched region. The scatter is likely due, in most part, to errors in the determination of the eq_{expt}, including such factors as whether or not the impurities were in substitutional sites. Detailed trends in the ξ_d, if any, are masked by this scatter. The ξ_d for Re and Os hosts are well defined, as are the eq_{expt} on which they are based. They increase in magnitude on going left from Au to Lu. Note that, except for Lu, Hf, and Ta impurities, these ξ_d take on a roughly constant value.

Second, the ξ_d for Fe and Ru impurities, as shown in the figure, nicely overlie those for Os, the $5d$ element from the same column of the Periodic Table. In addition (not shown), measurements of the quadrupole interaction have been recently reported[31] for Zr, the $4d$ counterpart of Hf, in Hf and Re hosts from which ξ_d values of ± 0.28 and ± 0.30 may be inferred using the eq_d of Table I. Assuming that these have signs consistent with the other impurities in these hosts, these ξ_d nicely overlap the ξ_d for Hf impurities. In other words, given this normalization the data for all impurities, $3d$, $4d$, and $5d$, display common behavior.

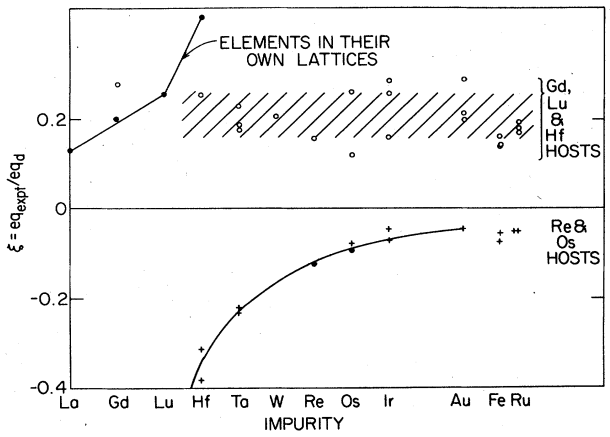

FIG. 6. Normalized field gradients, i.e., the ξ_d of Eq. (4) assuming that intra-atomic contributions dominate, for the $5d$ elements in various $5d$ hosts. A point for Lu in Re lies off the figure at $\xi_d = -0.93$. The solid circles indicate data for an element in its own host lattice, while the open circles denote impurity data where the left-hand elements, Gd, Lu, and Hf, are hosts; the pluses denote data where the right-hand Re and Os are hosts. The hatched region indicates where the data for the left-hand hosts is centered. Data, similarly normalized, is shown for Fe and Ru in the same hosts. For clarity, the parentheses of Figs. 2–4, indicating data for which the signs are unknown, are not shown here.

The third feature of Fig. 6 to be noted is that the ξ are quite substantial. A ξ_d of, say, $+0.2$, corresponds to having an aspherical d density corresponding to an excess of 0.2 of an electron's worth of $m_l=0$ d-orbital charge along the c axis, or, equivalently, a deficit of the same magnitude in the $m_l=2$ character in the vicinity of the hcp lattice's basal plane. Owing to the electron-electron Coulomb interaction, it is energetically favorable to have the valence charge spherically arranged within an atomic site. Bonding (and the associated band filling) introduces deviations from sphericity, but the nonzero ξ_d of concern here are a measure of the *difference* in bonding between the nearest neighbors in the basal plane and those above and below the plane. Granted that the neighbors are almost equidistant,[32] ξ_d values greater than ~ 0.2 in magnitude are "large." The ξ_d for Lu in Re is so large as to suggest that valence p-electron effects are significant. The intra-atomic Sternheimer antishielding factor R_d was not accounted for in the construction of Fig. 6. Its inclusion in the denominator of Eq. (4) would reduce the ξ_d by 30% at most, i.e., calculations of R_d for $5d$ elements[12,16] give $R_d \sim -0.3$, so that $1-R_d \sim 1.3$. Because $|R_d|$ is small, any variation in R_d, across the row, would have a modest effect on the normalization.

An alternate atomic scaling may be tried on the experimental gradients. Namely, assuming that they are primarily associated with q_{inter}, they may be divided by $\alpha(1-\gamma_\infty)$. Here, α is a fraction somewhere between one-third and two-thirds,[17] thus accounting for the reduction in the antishielding due to having the source of the gradient coming from the atoms which are immediate neighbors of the impurities (see Sec. II). The gradients are so scaled in Fig. 7, assuming a constant value of α $(=\frac{1}{2})$ for all the data and using the γ_∞ obtained with Eq. (6b). Both branches of the data display upward slopes with the leftmost impurities, Lu and Hf having the most negative scaled gradients when in the right-hand hosts, and right-hand impurities (such as Ir and Au) having the largest positive gradients when in the left-hand hosts. Details of the plotted trends, of course, depend on the assumption that α is a constant. Since α is expected to vary somewhat across the row, these plotted slopes will change a little. Scaled gradients are also shown for the Fe, Zr, and Ru impurity data. These use Sternheimer antishielding factors of -9.1 for Fe (Ref. 15) and interpolated values of -33 and -24 based on calculations (Ref. 19) for Zr and Ru, respectively. The Zr and Ru points overlap those for their $5d$ counterparts, Hf and Os, reasonably well, while those for Fe do not. It is possible, although improbable, that the Fe discrepancies are due either to the need of employing a different scale factor, α, for Fe, or to inconsistencies in the calculated γ_∞ values.

The ratios plotted in Fig. 7 are not normalized in the sense of the ξ_d of Fig. 6. To define the analog of a ξ factor requires an estimate of some sort of "standard" quadrupolar field due to the external source which would then be divided into the ratios plotted in Fig. 7. Assume, for example, that eq_{inter} arises primarily from charge transfer between the impurity and its nearest neighbors. Of course, the gradient arises primarily from the *difference* in such transfer to neighbors in the basal plane versus those out of the plane. The gradient, for an undistorted host lattice, associated with total excess charge Ne centered on the six coplanar neighbor sites, is

$$eq_{\text{inter}}(10^{17}\ \text{V/cm}^2) = -\frac{1.44Ne}{[a(\text{Å})]^3}\ , \tag{7}$$

where a is the hcp in-plane lattice constant. The N may be defined by assuming the experimental gradients are entirely due to this inter-atomic term, i.e.,

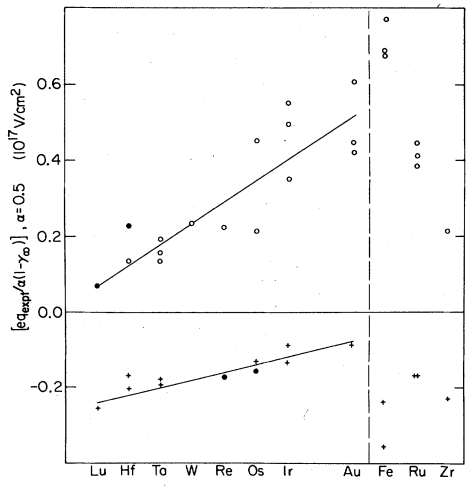

FIG. 7. Scaled field gradients where the external Sternheimer antishielding factor has been divided into the observed gradient for the $5d$ elements and Fe, Ru, and Zr in various $5d$ hosts. Points have been drawn with the same symbols as in Fig. 6 and the lines have been drawn to guide the eye.

$$Ne=\frac{-eq_{\text{inter}}a^3}{1.44}=\frac{-eq_{\text{expt}}}{\alpha(1-\gamma_\infty)}\frac{a^3}{1.44}\ . \tag{8}$$

Then the N maybe directly compared with the ξ_d of Fig. 6. Values of eq_{inter}/N range from $0.03(10^{17}$ V/cm$^2)$ to $0.07(10^{17}$ V/cm$^2)$ for Gd to Os, respectively. Dividing these quantities into the plotted ratios of Fig. 7 yields values of Ne, in the manner of Eq. (8), ranging from $1.5e$ to $20e$ in magnitude. These are huge. The smallest values are associated with Au and Ir in Re and Os hosts, and the largest with the same impurities in the left-hand hosts (N values approaching 30 are associated with Fe in these hosts). This estimate assumes a transfer of charge from the impurity to the six basal neighbors (i.e., a charge $Ne/6$ on each). Charge transfer of this sort is inconsistent with the fact that the quadrupole fields for atoms in their own lattices generally fall on the same curves as the impurity data. An alternative model is to presume that charge is concentrated angularly along bond lines rather than involving site charge transfer. Granted that the inter-atomic term involves charge outside the impurity site, it must be centered, radially, at something like three-fourths of the near-neighbor distance. Again, assuming that we are dealing with an imbalance of bonding charge along lines with neighbors in the basal plane, Eqs. (7) and (8) may be employed, providing that the a is replaced by $3a/4$. Estimates of Ne become $(\frac{3}{4})^3$, or ~ 0.4 times the values obtained above, and are, roughly speaking, an order of magnitude larger than their ξ_d counterparts. This suggests a variant of the Raghavan-Kaufmann conjecture.[10] From simple arguments associated with the continuity of electron density, one expects that if charge is concentrated along some bond line within the impurity cell, it is concentrated along the same line outside as well. If one further assumes that there are roughly equal amounts of this charge on one end of the bond as on the other (i.e., inside and outside the impurity cell), one can compare Eqs. (3a) and (7), or the values deduced for ξ_d and N, to conclude

$$\frac{eq_{\text{intra}}}{(1-\gamma_\infty)eq_{\text{inter}}}=K\ , \tag{9}$$

where K is roughly constant and $\sim +10$ for the alloys of concern here. The reversal in sign upon going from left to right-hand hosts is then associated with the reversal in sign of both terms.

The discussion above has neglected the host-lattice distortions and valence p-electron contributions. While significant host-lattice distortions are associated with a number of the alloy systems, such as Lu embedded in Os and vice versa, lattice distortions are not responsible for certain main features of Figs. 1–6. For example, some of the data contributing to the trends, such as those for elements in their own lattices, are for undistorted lattices. More important is the issue of valence p-electron contributions to the gradients, as was discussed in Sec. II. Evaluation of Eq. (4) for the $6p$ electrons of the $5d$ elements yields ξ_p values which are ~ 0.1 in magnitude for Lu in right-hand hosts and for Au in left-hand ones, and which, otherwise, are typically 0.01 to 0.05 in magnitude. Tiny amounts of aspherical p charge are of experimental significance, and the possibility of this, particularly of varying p contributions, is the major impediment to inferring trends in alloy bonding from the observed gradients. The discussion in the next section assumes that there are not marked variations in the amount of aspherical p character from one alloy to another.

V. BONDING TRENDS

Experimentally observed field gradients provide a measure of aspherical bonding effects, be they associated with charge transfer or with valence charge concentrated along directional lines. The fact that the eq_{expt} tend to fit in the same trends, for *both* impurities and host atoms, would indicate that it is directional bonding effects which predominate. Furthermore, this fact suggests that, while host-lattice distortions do occur in the immediate vicinity of an impurity, these distortions are not responsible for the gross trends in the observed eq_{expt}.

The raw data of Figs. 2–5 indicates that, to a remarkable extent, the gradients follow one of two trends depending on whether the host metal has under- or over-half-filled d bands. Wortmann and co-workers have shown[9] the similarity in Re- and Os host data and this has been shown to be applicable to yet other hosts. The positive field gradients of the left-hand (i.e., under-half-filled d-shell) hosts is indicative of excess valence-electron charge normal to the hcp basal plane (or, if you will, a deficit in the plane), while the reverse holds for the right-hand hosts. There are few exceptions, e.g., Ir and Au in Ti, which do not follow the main trend and of which more will be said shortly. The extent to which the trend is obeyed is surprising. For example, the bonding of the rare earths and Sc, Y, and Lu with the right-hand metals is different than the bonding of Ti, Zr, and Hf with the same metals, yet the effects measured by eq_{expt} are much the same for the two groups of hosts. Furthermore, the right-hand hosts come from three columns of the Periodic Table, yet the eq_{expt} for a given impurity in them are essentially the same.

We have, in general, assumed that the normalized gradients vary smoothly with position in the Periodic Table and that any deviations from smooth trends are due either to experimental details, such as samples where the impurities are not substitutional, or to inadequate knowledge of the factors involved in normalization. It is possible, and even likely, that there are real deviations from such smooth trends. Such devations are of interest but have not as yet been clearly demonstrated.

Inspection of the normalized results considered in the preceding section would suggest that the observed gradients, by their very magnitude, must be largely intra-atomic in origin. Granted this, and assuming that the gradients are primarily associated with d-band electrons, Fig. 6 may be inspected for chemical trends. There is considerable scatter in the ξ_d of the left-hand hosts, but, for example, it seems to make little difference whether it is Gd to the left or Ir well to the right which is implanted in Lu: both have essentially identical normalized gradients. Once atomic effects are normalized out, the observed gradients for the left-hand hosts are insensitive to either which host or what impurity is involved. The scatter is less for the right-hand hosts and here there is a

clear suggestion of a chemical trend. The gradients increase in magnitude, in a way which seems to track the strength of bonding, as the impurities are traversed from Au to Lu. However, the enthalpies of formation of the 50 at.%—50 at.% alloys show[33] a reversal upon going from Hf to Lu; that is, the enthalpies are smaller when Lu, as opposed to Hf, is alloyed with elements to the right. Except for this reversal, the ξ_d associated with the right-hand hosts appear to mimic the trends in cohesion. Consider Sc and Ti, which are the $3d$ counterparts of Lu and Hf. Their 50 at.%—50 at.% alloy enthalpies show[33] those for Sc to be larger than those for Ti, i.e., they do not show the reversal seen for Lu and Hf. It would be of interest to compare the trend in the Sc and Ti impurity-site gradients with that seen for Lu and Hf. This disparity in bonding behavior may also be reflected in the fact that the gradients for Ir and Au in Ti hosts (and Ir in Zr also) do not follow the main trend in gradient behavior. They instead display "intermediate" behavior with normalized gradients which are weaker (and, in some cases, those with Sc as host are greater) than those associated with the other left-hand hosts. Some features of the normalized eq_{expt} thus seem to reflect bonding trends.

The main shortcoming of the above discussion is that it neglects the possibility of valence p-electron contributions to the gradients. The very large magnitudes of the gradients observed, particularly, for Lu in Re, suggest that these contributions are not negligible. It is not generally appreciated how huge these may be, as is illustrated by the eq_p of Table I (note that since these vary by about a factor of 2, the associated ξ_p resemble a modestly distorted version of Fig. 2). While potentially important to the observed gradients, such aspherical p-electron charge is much less important to both the energetics of alloy formation and to the gross shape of the valence charge around an atomic site.

VI. CONCLUSION

We have considered the systematics of the electric-field-gradient behavior of transition-metal impurities in transition-metal hosts utilizing essentially all the available experimental data. Several schemes were applied to normalize the electric field gradients so as to remove the effects intrinsic to the atomic hyperfine properties of the impurity. This involved renormalized-atom estimates of effective valence-electron field gradients, i.e., the eq_d and eq_p of Eqs. (3). In addition, Sternheimer antishielding factors, γ_∞, were required for elements for which they are not available. This led to the observations, in the Appendix, concerning how γ_∞ scales with the size of the atom in question. It was shown that the normalized gradients fall into a pattern. Fe, Zr, and Ru, the only $3d$ and $4d$ impurity elements for which there are data, display the same behavior as the $5d$ impurities. For Fe, this required adopting the new value of the ^{57}Fe nuclear quadrupole moment obtained[27] by Duff and co-workers. The large magnitudes of the gradients imply that they are primarily intra-atomic, not inter-atomic, in origin, and that valence p-electron contributions are very likely important.

Whatever the source—primarily d, substantially p, or inter-atomic—there is the one striking feature of the observed gradients. That is that the gradients follow two trends, differing in sign, depending on whether the host has over or under-half-filled d bands. It would be nice, if it were possible, to trace the trends through the metals (Cr, Mo, W, V, Nb, and Ta) which lie between the two groups of hosts, but these metals are, of course, cubic. The difference in sign of the eq_{expt} is not due to a difference in hcp c/a ratios, but is a real measure of the tendency of bonding charge to lie on or away from the basal plane. This tendency can be investigated by energy-band calculations for elemental metals from each of the groups of hosts. There are indications of at least a few deviations from the main trends and these main trends show but weak chemical dependence. These issues deserve further experimental investigation. The nuclear moments are not all sufficiently well known (Hf comes to mind). It would be desirable to know more signs of the gradient, at least in selected cases. In addition, it would be useful to have more data for $3d$ and $4d$ impurities, perhaps Sc, Ti, and Zr.

ACKNOWLEDGMENTS

The work done at Brookhaven National Laboratory was supported by the Division of Materials Sciences, U.S. Department of Energy, under Contract No. DE-AC02-76CH00016.

APPENDIX

A set of γ_∞ values are required in Sec. IV for the $5d$ metal atoms, and, while there are a number of estimates, many omit the contributions from the $5d$ shell. This has led to the use of an interpolation scheme based on the fits which are described here. The fits are relevant to the way γ_∞ varies in various sequences of ions in general. These fits assume that the external Sternheimer antishielding factor depends on the size of the atom as

$$\gamma_\infty = bR^n = b'V^{n/3}, \tag{A1}$$

where R will be taken to be the Pauling-type radius as defined[25] by Slater and V is the atomic volume. The exponent n will be seen, on the average, to have the value $\sim +4.5$ for the cases studied here. There are deviations which are substantial, and these occur in a systematic way. In fact, it is concluded that a smaller exponent is applicable to the sequence of $5d$ elements. The point is that γ_∞ does depend on ion size, and Eq. (A1) is useful when extrapolating from one ion to another.

Values of γ_∞ and of the Slater radii are listed for several sequences of ions in Table II. Omitted from the list are those first-row elements, such as Li^+, which have no valence p shells because it is the valence p and d shells which are primarily responsible for the antishielding. Lacking such shells the antishielding of the first-row elements is not comparable with that of the others. Consider the alkali metal ions and, in particular, the largest and smallest of these. Taking Eq. (A1), we have

$$\frac{\ln[\gamma_\infty(Cs^+)/\gamma_\infty(Na^+)]}{\ln[R(Cs^+)/R(Na^+)]} = n = 4.49. \tag{A2}$$

TABLE II. Sternheimer antishielding factor γ_∞ and the Slater radii R for four sequences of ions. The γ_∞ come from Refs. 15, 16, 18, and 19, and the radii from Ref. 25.

Ion	γ_∞	R (Å)
Na^+	−4.56	0.95
K^+	−17.32	1.33
Rb^+	−47.2	1.48
Cs^+	−102.5	1.90
Mg^{2+}	−3.350	0.65
Ca^{2+}	−13.95	0.99
Sr^{2+}	−41.35	1.13
Ba^{2+}	−94.23	1.35
F^-	−22.53	1.36
Cl^-	−56.6	1.81
Br^-	−123.0	1.95
Cu^+	−17.29	1.35
Ag^+	−34.87	1.60
Au^+	−74.2	1.35[a]

[a]This radius is inconsistent with those for Cu^+ and Ag^+ and should not be employed in the present fits.

Equivalent fits across the other sequences of ions yield the results listed in Table III. All yield values of n which are close to 4.5.

This would suggest, on the average, a simple scaling rule for the effect of atomic size on antishielding factors, namely

$$\gamma_\infty \propto V^{1.5} . \tag{A3}$$

However, detailed fits of adjacent pairs of ions in the three main sequences in Table II yield

$$\begin{aligned} &n(2p-3p)\sim 3 \text{ to } 4 , \\ &n(3p-4p)\sim 8 \text{ to } 9 , \\ &n(4p\sim 5p)\sim 3 \text{ to } 4 , \end{aligned} \tag{A4}$$

where $n(2p-3p)$ results from fitting the pair of $2p$ and $3p$ ions in the same sequence. While there is a considerable spread in n, there is also a well-defined pattern in the values which depends on the electron shells involved. The large value of n occurs upon going from the $3p$ to the $4p$ elements, and this is associated with the shielding due to the introduction of the first closed d shell in the ion core, the $3d$, in the $4p$ atoms. This large n is thus due to other than size effects. The introduction, first, of a d core shell (and later, with the heavy elements, of an f) has repercussions[34] on potentials and, in turn, on alloying properties such that they do not vary in a smooth way as one alloy component is replaced by another coming from the same column of the Periodic Table. It would appear that an exponent closer to 3 than to 4.5 is, as a rule, more suitable for insertion in Eq. (A1).

TABLE III. Coefficients b and exponents n in Eq. (A1) for $-\gamma_\infty$ $(=bR^n)$ for the four sequences of ions considered in the Appendix.

Ion sequence	b	n
Na^+–Cs^+	5.741	4.49
Mg^{2+}–Ba^{2+}	23.94	4.56
F^-–Br^-	5.297	4.71
Cu^+–Ag^+	5.007	4.13

The estimates in Sec. II for γ_∞ values for the $5d$ elements also involve, following Eqs. (6), an estimate of the varying contribution from the open $5d$ shell due to the varying $5d$ occupation. Values were obtained by extrapolating off the calculated value for Au using n values of both 4.5 and 3.0. The extrapolated values differ substantially for only Lu and Hf, which are much larger than the other $5d$ elements. Comparison with calculated values for W and for some of the heavier rare-earth elements suggests that $n=3.0$ is the better choice.

One expects n to be a positive quantity. Granted that the source of the lattice potential comes from outside the ion, that potential perturbs the ion as

$$V \propto r^2 P_2(\cos\theta) , \tag{A5}$$

where $P_2(\cos\theta)$ is a Legendre function. Hence one might expect $n=2$. Remember that the Sternheimer antishielding factor γ_∞ is determined primarily by the values of $\gamma_\infty(np\rightarrow p)$ and $\gamma_\infty(n'd\rightarrow d)$ for the outermost occupied np and $n'd$ shells. In fact, $\gamma_\infty(nl\rightarrow l)$ is given by[10–13]

$$\gamma_\infty(nl\rightarrow l)=C_l \int_0^\infty u_0'(nl)u_1'(nl\rightarrow l)r^2 dr , \tag{A6}$$

where C_l is an angular integral which depends on l only, and $u_0'(nl)$ is the unperturbed, normalized, radial wave function of the nl shell (times r).

The perturbation $u_1'(nl\rightarrow l)$ is the solution of the following inhomogeneous radial equation which was introduced by Sternheimer[13] in 1951:

$$\left[-\frac{d^2}{dr^2}+\frac{l(l+1)}{r^2}+V_0-E_0\right]u_1'(nl\rightarrow l) = u_0'(nl)\left[\frac{1}{r^3}-\left\langle\frac{1}{r^3}\right\rangle_{nl}\right] . \tag{A7}$$

In addition, we have the orthogonality condition for $u_1'(nl\rightarrow l)$, namely[13]

$$\int_0^\infty u_0'(nl)u_1'(nl\rightarrow l)dr=0 . \tag{A8}$$

The orthogonality condition on u_1' introduces an extra node into it, causing it to be more extended radially than u_0', and while this cannot be shown analytically, this apparently leads to n values in excess of 2.

[1]R. E. Watson, L. J. Swartzendruber, and L. H. Bennett, Phys. Rev. B **24**, 6211 (1981).
[2]E. Hagn, M. Zahn, and E. Zech, Phys. Rev. B **28**, 3130 (1983), and earlier references cited therein.
[3]F. E. Wagner, Hyperfine Interact **13**, 149 (1983).
[4]H. C. Verma, J. Chappert, and G. N. Rao, Hyperfine Interact. **11**, 45 (1981).
[5]J. Kotthaus and R. Vianden, Hyperfine Interact. **14**, 99 (1983).
[6]H. Ernst, W. Koch, F. E. Wagner, and E. Bucher, Phys. Lett. **70A**, 246 (1979).
[7]There is a disparity in the quoted eq_{expt} from various sources, and the results quoted in Refs. 2–6 are presumed to supersede other data. The remainder of the experimental results have been taken from the tabulations of Refs. 8 and 9.
[8]W. Witthuhn and W. Engel, in *Hyperfine Interactions of Radioactive Nuclei,* edited by J. Christiansen (Springer, Berlin, 1983); R. Vianden, Hyperfine Interact. **16**, 1081 (1983).
[9]G. Wortmann, B. Perscheid, G. Kaindl, and F. E. Wagner, Hyperfine Interact. **9**, 343 (1981).
[10]R. S. Raghavan, E. N. Kaufmann, and P. Raghavan, Phys. Rev. Lett. **34**, 1280 (1975); P. Raghavan, E. N. Kaufmann, R. S. Raghavan, E. J. Ansaldo, and R. A. Naumann, Phys. Rev. B **13**, 2835 (1976).
[11]See, e.g., T. P. Das and M. Pomerantz, Phys. Rev. **123**, 2070 (1961).
[12]R. M. Sternheimer, Phys. Rev. **80**, 102 (1950); **95**, 736 (1954); **105**, 158 (1957); **146**, 140 (1966); **164**, 10 (1967); R. M. Sternheimer and R. F. Peierls, Phys. Rev. A **3**, 837 (1971); **4**, 1722 (1971); R. M. Sternheimer, *ibid.* **6**, 1702 (1972); **9**, 1783 (1974).
[13]R. M. Sternheimer, Phys. Rev. **84**, 244 (1951).
[14]H. M. Foley, R. M. Sternheimer, and D. Tycho, Phys. Rev. **93**, 734 (1954); R. M. Sternheimer and H. M. Foley, *ibid.* **102**, 731 (1956); R. M. Sternheimer, *ibid.* **132**, 1637 (1963).
[15]R. M. Sternheimer, Phys. Rev. **130**, 1423 (1963).
[16]R. M. Sternheimer, Phys. Rev. **146**, 140 (1966); **159**, 266 (1967).
[17]A. C. Beri, T. Lee, T. P. Das, and R. M. Sternheimer, Phys. Rev. B **28**, 2335 (1983).
[18]R. P. Gupta, B. K. Rao, and S. K. Sen, Phys. Rev. A **3**, 545 (1971); R. P. Gupta and S. K. Sen, Phys. Rev. A **7**, 850 (1973); **8**, 1169 (1973).
[19]F. D. Feiock and W. R. Johnson, Phys. Rev. **187**, 39 (1969).
[20]R. E. Watson, A. C. Gossard, and Y. Yafet, Phys. Rev. **140**, A 375 (1965).
[21]See, e.g., M. Piecuch and C. Janot, Hyperfine Interact. **11**, 13 (1981).
[22]See, e.g, W. D. Knight, in Solid State Physics, edited by F. Seitz and D. Turnbull (Academic, New York, 1956), Vol. 2, p. 93; L. H. Bennett, R. W. Mebs, and R. E. Watson, Phys. Rev. **171**, 611 (1968).
[23]See, e.g., V. L. Moruzzi, J. F. Janak, and A. R. Williams, *Calculated Electronic Properties of Metals* (Pergamon, New York, 1978).
[24]T. K. Sham, R. E. Watson, and M. L. Perlman, in *Mössbauer Spectroscopy and Its Chemical Applications,* edited by J. G. Stevens and G. K. Shenoy (American Chemical Society, Washington, D.C., 1981).
[25]J. C. Slater, Quarterly Progress Report No. 46, Solid-State and Molecular Theory Group, Massachusetts Institute of Technology, 1962 (unpublished).
[26]M. E. Rose, J. Math. Phys. **37**, 215 (1958). For an example where the contributions from surrounding multipoles to the spherical potential at a site is estimated, see Appendix C in L. Hodges, R. E. Watson, and H. Ehrenreich, Phys. Rev. B **5**, 3953 (1972).
[27]K. J. Duff, K. C. Mishra, and T. P. Das, Phys. Rev. Lett. **46**, 1611 (1981).
[28]S. Vajda, D. G. Sprouse, M. H. Rafailovich, and J. W. Noé, Phys. Rev. Lett. **47**, 1230 (1981).
[29]For example, the eq_{expt} for Ir, Ru, and, to some extent, Fe (although not Gd, Hf, Ta, and Au) in Sc as the host lie significantly higher than do the surrounding eq_{expt} in Figs. 3–5. This suggests the occurrence of a different class of impurity behavior for these elements in Sc. In fact, in the case of Ir and Ru the gradients are so large as to suggest that the sites must have lower symmetry than do the substitutional sites. Recently, Forker *et al.* [M. Forker, S. Scholz, and L. Freise, Hyperfine Interact. **15**, 783 (1983)] reported two gradients for Ru in Sc, hence the two points in Fig. 4. Previously only the eq_{expt} of larger magnitude had been observed. From the variation in intensity with impurity concentration, they concluded that the newly observed eq_{expt}, of smaller magnitude is the one associated with substitutional sites. Both eq_{expt} values are at variance with the gradients associated with Ru in other hosts.
[30]It should be noted that large gradients, hence large ξ, are reported for Hf in various $3d$ and $4d$ hosts, as well as in Hf metal (see Fig. 5). Note, also, the large negative ξ for Hf in Re and Os hosts in Fig. 6. It is difficult to say whether this is due to alloying effects or to incorrect eq_{expt} (due, for example, to a wrong assignment of nuclear quadrupole moments).
[31]P. Raghavan, R. N. Saxena, C. S. Lee, and R. S. Raghavan, Abstracts to the 1983 Gröningen Meeting on Hyperfine Interactions (unpublished).
[32]It might be noted that the nearest neighbors lying outside the basal plane of the hcp structure lie closer than those in the plane for all the undistorted host lattices of concern here; hence the reversal in sign of eq_{expt} for the two groups of hosts is not due to a difference in bonding strength associated with the relative proximities of the two sets of sites.
[33]R. E. Watson and L. H. Bennett, CALPHAD **8**, 307 (1984), in particular, Fig. 4.
[34]See, e.g., L. H. Bennett, R. W. Mebs, and R. E. Watson, Phys. Rev. **171**, 611 (1968); R. E. Watson, L. H. Bennett, and J. W. Davenport, Phys. Rev. B **27**, 6428 (1983).